



# Influence of Sintering Temperature on Phase Formation and Superconducting Properties of $\text{Bi}_2\text{Sr}_2\text{CaCu}_2\text{O}_{8+\delta}$ via Thermal Treatment Method

Rahayu Emilia Mohamed Khaidir<sup>1</sup>, Aliah Nursyahirah Kamarudin<sup>1</sup>, Mohd Mustafa Awang Kechik<sup>1\*</sup>, Chen Soo Kien<sup>1</sup>, Lim Kean Pah<sup>1</sup>, Muhammad Kashfi Shabdin<sup>1</sup>, Muhammad Khalis Abdul Karim<sup>1</sup>, Aris Doyan<sup>2</sup>, Abdul Halim Shaari<sup>1</sup>

<sup>1</sup>Superconductor & Thin Films Laboratory, Department of Physics, Faculty of Science, Universiti Putra Malaysia, 43400 UPM Serdang, Selangor, Malaysia

<sup>2</sup>Physics Education Program, FKIP, University of Mataram, Indonesia

Received: February 13, 2025

Revised: March 22, 2025

Accepted: April 25, 2025

Published: April 30, 2025

Corresponding Author:

Mohd Mustafa Awang Kechik

[mmak@upm.edu.my](mailto:mmak@upm.edu.my)

© 2025 The Authors. This open-access article is distributed under a (CC-BY License)



**Abstract:** High-temperature superconductor  $\text{Bi}_2\text{Sr}_2\text{CaCu}_2\text{O}_{8+\delta}$  (Bi-2212) was successfully prepared using a thermal treatment method, starting with nitrate-based precursors. This study focused on how different sintering temperatures affect the material's critical temperature,  $T_c$ . The process began with a pre-calcination step at 600 °C for 12 hours, followed by calcination at 820 °C for 24 hours. After that, the powder was pressed into pellets and sintered at 830 °C, 840 °C, 850 °C, and 860 °C, each for 24 hours. The  $T_{c\text{-onset}}$  values increased with sintering temperature, reaching 50 K at 830 °C, 65 K at 840 °C, and 78 K at 850 °C. SEM images showed closely packed, flake-like grains around 2  $\mu\text{m}$  in size, while XRD analysis confirmed that the sample sintered at 850 °C had the highest Bi-2212 phases as a major phase. Thus, this work outlines the practical steps of the thermal treatment approach and shows how adjusting the sintering temperature can significantly influence the superconducting performance and phase formation of Bi-2212.

**Keywords:**  $\text{Bi}_2\text{Sr}_2\text{CaCu}_2\text{O}_{8+\delta}$ ; Critical temperature; Phase formation; Sintering; Thermal treatment

## Introduction

Bismuth-based high-temperature superconductors (BSCCO), particularly the  $\text{Bi}_2\text{Sr}_2\text{CaCu}_2\text{O}_{8+x}$  (Bi-2212) phase, have gained significant attention due to their relatively high critical temperature,  $T_c$  and potential for practical applications such as superconducting DC cables, superconducting energy storage systems (SMES), magnetic levitation trains and superconducting tokamak magnet systems (Adetokun et al., 2022; Cheng et al., 2021; Matsushita et al., 2021; Zhai et al., 2022). In the late 1980s, Bi-2212 exhibited a  $T_{c\text{-onset}}$  around 95 K and has been extensively studied for its layered perovskite structure and superconducting properties (Dogruer et

al., 2021; Kechik et al., 2008; Maeda et al., 1993). Its ability to carry high current densities and compatibility with various fabrication techniques make it a promising candidate for technological applications (Abdullah et al., 2023; Sharma et al., 2013; Siregar et al., 2021).

The superconducting properties of Bi-2212 are highly sensitive to processing conditions, particularly the sintering temperature (Sukor et al., 2024). Variations in sintering temperature can influence phase formation, grain connectivity, and oxygen content, all of which are critical factors affecting  $T_{c\text{-onset}}$  and overall superconducting performance (Tsukamoto et al., 1994). Previous studies have demonstrated that optimizing the sintering temperature can enhance the phase purity and

## How to Cite:

Khaidir, R. E. M., Kamarudin, A. N., Awang Kechik, M. M., Kien, C. S., Pah, L. K., Shabdin, M. K., ... Shaari, A. H. (2025). Influence of Sintering Temperature on Phase Formation and Superconducting Properties of  $\text{Bi}_2\text{Sr}_2\text{CaCu}_2\text{O}_{8+\delta}$  via Thermal Treatment Method. *Journal of Material Science and Radiation*, 1(1), 1-6. Retrieved from <https://journals.balaipublikasi.id/index.php/jmsr/article/view/359>

crystallinity of Bi-2212, leading to improved superconducting characteristics (Arlina et al., 2015). However, achieving the optimal balance between these factors remains a challenge.

Therefore, this study aims to investigate the effects of different sintering temperatures on the superconducting properties of Bi-2212 superconductors. By systematically varying the sintering temperature and analyzing the resulting structural and superconducting characteristics, we seek to identify the optimal conditions for maximizing  $T_{c-onset}$  and phase purity. The thermal treatment method will be employed for sample preparation, which has been used in producing BSCCO and REBCO superconductors, thus offering advantages such as better homogeneity and lower processing temperatures compared to conventional solid-state methods (Dzul-Kifli et al., 2022; Kamarudin et al., 2022; Dihom et al., 2017). Understanding the relationship between sintering temperature and superconducting properties is crucial for advancing the practical applications of Bi-2212 superconductors.

## Method

Bi-2212 samples were prepared using the thermal treatment method with metal nitrate based on the desired stoichiometric equation of a 2:2:1:2 ratio. The mixed powder was weighed and dissolved in 100 ml of deionised water with 3g of polyvinyl pyrrolidone (PVP) which acts as a stabilizer (Zahari et al., 2017). Then, the mixed solution was stirred using a magnetic stirrer with 850 revolutions per minute (rpm) at 80 °C for 2 hours. The mixed solution was poured into the glass petri dish and dried in an oven for 2 hours at 90 °C until it turned into a green solid-like texture. The mixed powders were ground in a mortar and pestle to ensure the homogeneity of the powders for 2 hours. Then, the obtained powders underwent a calcination process twice at 600 °C and 850 °C for 4 hours and 24 hours, respectively, with intermediate grinding. The powdered samples obtained from the calcination process were pressed into a circular pellet of 1 g with a 13 mm diameter and 5 mm thickness. In this study, the sintering temperature of Bi2212 sample pellets was varied to find the optimum sintering temperature of Bi2212 samples. Thus, the sintering temperatures were varied at 830 °C, 840 °C, 850 °C and 860 °C for 24 hours with the heating rate of 2 °C/h. Then, the obtained Bi2212 samples were measured using several characterisations. The phase formation of Bi2212 was analysed using PAN Analytical X'Pert Pro MPD X-Ray Diffractometer (Philips) with  $\text{CuK}\beta$  radiation over angle  $2\theta = 20^\circ - 80^\circ$ . The surface morphology and topography of Bi2212 samples were observed through a scanning electron microscope

(SEM). Lastly, the resistivity of the Bi2212 samples was determined at different sintering temperatures by using the four-point probe (4pp).

## Result and Discussion

Thermogravimetric analysis (TGA) was conducted to investigate the thermal decomposition behaviour of the BSCCO sample. Based on the TGA results, the appropriate calcination and sintering temperatures can be identified. As illustrated in **Figure 1**, the data strongly suggest that the optimal sintering temperature is above 835 °C. It was observed that a significant weight loss occurred during the initial stage, primarily due to the decomposition of the sample's constituents. Approximately 45% of weight loss, from 100% to around 55%, occurs in the first interval (Drop 1), which is mainly attributed to the evaporation of water at 100 °C. In the subsequent intervals, additional mass losses can be linked to the removal of residual water and the decomposition of minor impurities.

During the second stage (Drop 2), which occurs within the 200–400 °C range, copper nitrate begins to decompose into copper oxide, accounting for roughly 10% of the total weight loss. In the third stage (Drop 3), between 400–600 °C, bismuth nitrate undergoes decomposition to form bismuth oxide, contributing to a further weight reduction of approximately 5–8%. Finally, in the fourth interval (Drop 4), spanning from 600–800 °C, additional decomposition of bismuth nitrate and calcium nitrate takes place, resulting in the formation of bismuth oxide and calcium oxide, respectively. These thermal decomposition behaviors are consistent with those reported by the previous report (Abdullah et al., 2023; Kavitha et al., 2024; Sekkina & Elsabawy, 2002).

All samples were characterized by using XRD for phase formation identification to find the intensity over  $2\theta (\text{°}) = 20^\circ - 80^\circ$ . The XRD patterns were matched with the same ICSD, which are standard data files, and the analysis of the peaks that exist in those patterns was analysed by using X'Pert Highscore Plus software. From Figure 2, it shows that the XRD patterns for all sintering temperatures are almost the similar. Even though the samples were sintered with different sintering temperatures, the structures of all samples are the same, which are single phase and orthorhombic. From the plotted graphs below, the main peaks for all samples are the Bi-2212 phases. This proved that all samples are Bi-2212 bulk. From Table 1, it can be observed that the Bi-2201 phases decrease with sintering temperature up to 850 °C. This is due to the further formation of Bi-2212 phases as sintering temperature increases.

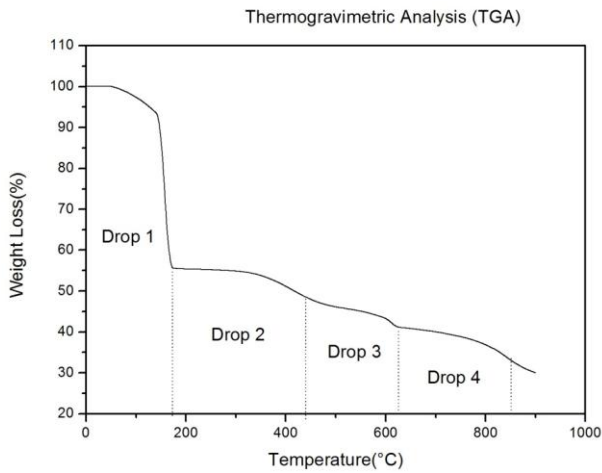


**Figure 1.** Graph of weight loss against temperature for the powder sample before the calcination process.

The phases of Bi-2212 increase from a sintering temperature of 830 °C to 840 °C, meanwhile, then the Bi-2212 phases decrease at a sintering temperature of 850 °C due to the new formation of Bi-2223 phases. Thus, the increase in sintering temperature from 830 °C to 850 °C will affect the phase formation of the BSCCO structure. Nevertheless, the lattice parameters of Bi-2212 at 850 °C were  $a = 5.371 \text{ \AA}$ ,  $b = 33.87 \text{ \AA}$  and  $c = 4.844 \text{ \AA}$  as tabulated in Table 1. This demonstrated that the size and shape of the unit cell of a crystal lattice, and also indicates that the Bi-2212 samples are orthorhombic, as the crystal system of orthorhombic is  $a \neq b \neq c$ , where the axes are preserved.

**Table 1.** The lattice parameter for all samples at different sintering temperatures.

Samples	Lattice Parameter			Volume of cell ( $\text{\AA}^3$ )
	$a$ ( $\text{\AA}$ )	$b$ ( $\text{\AA}$ )	$c$ ( $\text{\AA}$ )	
830 °C	5.39	30.84	5.40	897.49200
840 °C	5.40	30.84	5.40	900.38740
850 °C	5.37	33.87	4.84	881.14990

**Figure 3** presents the superconducting transition  $T_{c\text{-onset}}$  at which the resistance drops to zero, and the  $T_{c\text{-offset}}$  along with the transition width  $\Delta T_c$  for samples sintered at temperatures ranging from 830 °C to 850 °C. As tabulated in **Table 2**, the  $T_{c\text{-onset}}$  values for the samples sintered at 830 °C, 840 °C, and 850 °C are 50 K, 65 K, and 78 K, respectively. These results indicate a clear trend where  $T_{c\text{-onset}}$  increases with higher sintering temperatures. Notably, the highest  $T_{c\text{-onset}}$  of 78 K was achieved at a sintering temperature of 850 °C, which closely approaches the theoretical critical temperature of Bi-2212, reported as 80 K (Khalil & Sedky, 2005; Sugawara et al., 2018). The enhancement in  $T_{c\text{-onset}}$  with increasing sintering temperature can be attributed to the improvement of the crystallinity and grain connectivity

within the Bi-2212 phase (Sharma et al., 2013). A good grain alignment and densification reduce weak-link behavior at grain boundaries, facilitating more efficient superconducting current pathways and thereby improving the  $T_{c\text{-onset}}$  values (Arlina et al., 2015).

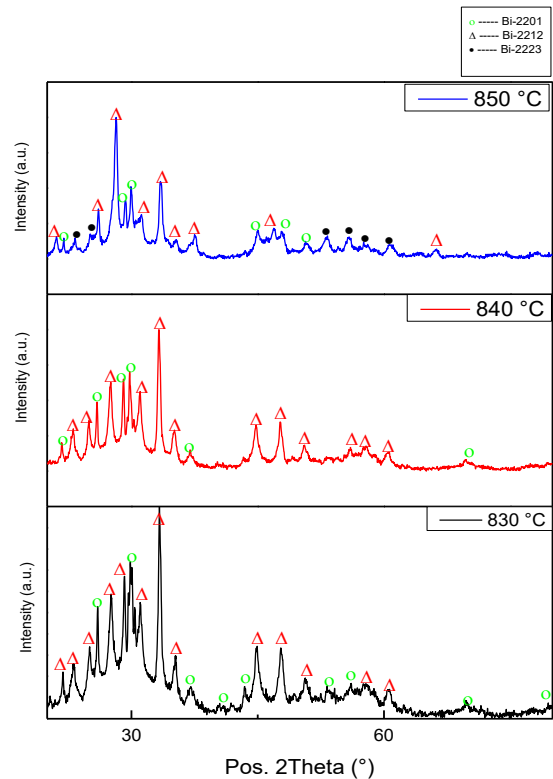


**Figure 2.** The graph of XRD patterns with different sintering temperatures of 830 °C, 840 °C and 850 °C.

Also, the increase in sintering temperatures can lead to an increase in the oxygen content within the crystal lattice (Hapipi et al., 2018). The oxygen content plays a crucial role in determining the carrier concentration in cuprate superconductors. Thus, an optimal oxygen content will help to enhance the hole doping in the  $\text{CuO}_2$  planes, which is essential for achieving higher superconducting transition temperatures (Kameli et al., 2006). Studies have shown that annealing Bi-2212 samples at higher temperatures can increase  $T_{c\text{-onset}}$  by improving oxygen ordering and reducing structural defects (Tsukamoto et al., 1994). Moreover, the elimination of secondary phases and impurities at higher sintering temperatures contributes to the purity and homogeneity of the superconducting phase. The presence of non-superconducting secondary phases can disrupt the superconducting network, leading to reduced  $T_{c\text{-onset}}$  values. Therefore, higher sintering temperatures facilitate the formation of a more homogeneous Bi-2212 phase, which is conducive to higher  $T_{c\text{-onset}}$ . Nevertheless, these findings are consistent

with previous studies that have reported similar enhancements in  $T_{c-onset}$  with increased sintering or annealing temperatures (Arlina et al., 2015).

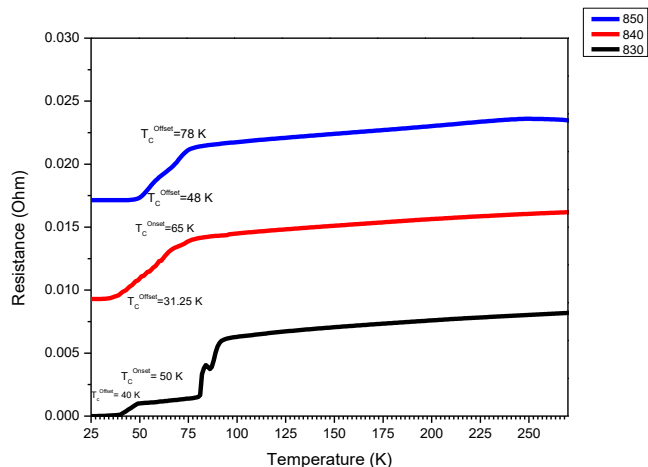


**Figure 3.** Graph of resistance against temperature at different sintering temperatures.

**Table 2.** Variation of  $T_{c-onset}$  (K),  $T_{c-offset}$  (K) and transition range,  $\Delta T_c$  for Bi-2212 phase with sintering temperature 830 °C, 840 °C and 850 °C.

Temperature (°C)	$T_{c-onset}$ (K)	$T_{c-offset}$ (K)	Transition width, $\Delta T_c$	Grain size ( $\mu\text{m}$ )
830	50.00	40.00	10.00	1.369
840	65.00	31.25	33.75	1.992
850	78.00	48.00	30.00	2.227

All samples prepared were then further closely viewed on the cross-section with magnification of 5000x. From the SEM micrograph shown in Figure 4, the grain size for the Bi-2212 samples was observed. The grain size was measured using the ImageJ software, and the average particle size of all samples was tabulated in **Table 2**. It was observed that the micrograph of the sample sintered at 830 °C showed that the grains were plate-like in form, strongly anisotropic and in a wide range of distribution. Also, the average grain size of the sample was observed, which is about  $\sim 1.37 \mu\text{m}$ . As sintering temperature increases up to 840 °C, the average grain size is about  $\sim 1.99 \mu\text{m}$ , and the shape becomes more irregular and larger. It shows that the average grain size is at its largest, which is about  $\sim 2.23 \mu\text{m}$ , when the sample is sintered at a temperature of 850 °C, and as the sintering temperature increases, the shape becomes more irregular and stronger as the grains become well-connected to each other. These results were reported similarly to the previous study (Abdullah et al., 2023). The increase in the sintering temperature from 820 °C up until 860 °C for 24 hours will increase the grain size of the Bi-2212 microstructure (Darsono et al., 2015).

In addition, from the SEM images, it can be observed that as sintering temperature increases, the grain boundaries between the grains decrease; thus, the particle size becomes larger and increases the average size of the grains (Abdullah et al., 2023). The grains become well connected to each other, and the phase of samples Bi-2212 starts to form well as the sintering temperature increases. For EDX analysis, four small areas were randomly picked on the image of the SEM with a magnification of 5000x for every sample. **Figure 5** presents the results of EDX spectra for Bi-2212 phases sintered at different sintering temperatures of 830 °C, 840 °C and 850 °C, respectively. From the figure, the real composition of Bi, Sr, Ca, Cu and O is displayed, neglecting the possibility of any impurity's existence in the samples. **Table 3** tabulates the ratio of the Bi-2212 phase at different sintering temperatures. It was observed that the ratio of Br: Sr: Ca: Cu is approximately 2:2:1:2 for all samples. In addition, the presence of the Bi-2212 phase as a major phase being produced was proved for samples heated at 830 °C to 850 °C.

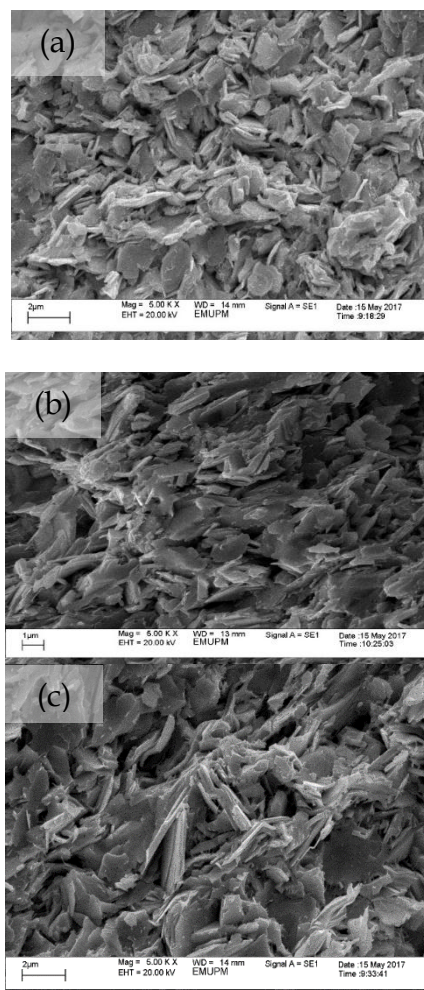


**Figure 4.** SEM image of Bi-2212 sintered at different sintering temperatures: a) 830 °C, b) 840 °C and c) 850 °C.

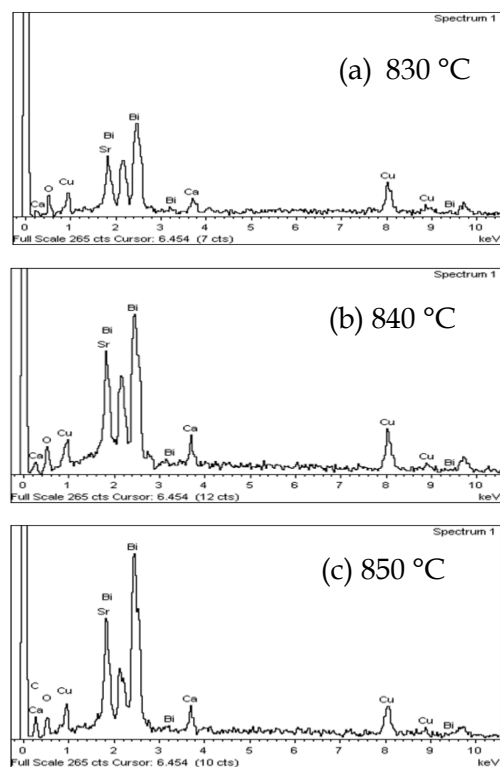


**Figure 5.** EDX analysis for Bi-2212 samples at different sintering temperatures (a) 830 °C, (b) 840 °C and (c) 850 °C.

**Table 3.** The ratio for the Bi-2212 phase at different sintering temperatures.

Temperature (°C)	Bi	Sr	Ca	Cu	O	Ratio
830	11.6	8.7	4.4	12.5	62.9	1.9: 2.0: 0.9: 2.0: 3.6
840	13.5	11.2	4.5	17.6	53.2	2.0: 1.7: 1.0: 2.6: 7.9
850	9.3	7.7	3.4	10.7	52.5	1.7: 2.2: 0.6: 2.0: 9.8

## Conclusion

In this study, the effects of different sintering temperatures on the superconducting properties of Bi-2212 samples prepared via the thermal treatment method were systematically investigated. The analysis of the structural and electrical properties revealed that sintering temperature plays a crucial role in enhancing phase formation, grain connectivity, and superconducting properties of  $T_c$  values. From the study, Bi-2212 samples sintered at 850 °C exhibited the most favourable superconducting performance, with a sharp transition and the highest  $T_{c-onset}$  value was observed. This suggests that 850 °C is the optimal sintering temperature for achieving a well-formed Bi-2212 phase with improved superconducting characteristics. The thermal treatment method has proven to be effective for synthesizing high-quality Bi-2212 superconductors. These findings provide valuable insights for optimizing the processing conditions of BSCCO materials, which are essential for their potential

application in superconducting devices and energy-related technologies. In conclusion, these findings confirm that careful control of sintering temperature is essential to enhance the superconducting performance of BSCCO materials.

## Acknowledgments

Authors gratefully acknowledge financial support from the Ministry of Higher Education Malaysia (MOHE) for the Fundamental Research Grant Scheme FRGS/1/2017/STG02/UPM/02/4 (5546036) Universiti Putra Malaysia.

## Author Contributions

Conceptualization, R.E.M.K., M.M.A.K. and A.N.K.; methodology, R.E.M.K.; software, A.N.K.; validation, C.S.K. L.K.P, A.D. and A.H.S.; formal analysis, R.E.M.K. and M.M.A.K.; investigation, R.E.M.K. and A.N.K.; resources, M.M.A.K.; data curation, R.E.M.K. and A.N.K.; writing—original draft preparation A.N.K. and R.E.M.K.; writing—review and editing, A.N.K., M.M.A.K. and A.D.; visualization, M.K.A.K and M.K.S.; supervision, C.S.K., L.K.P., A.D. and A.H.S.; project administration, M.M.A.K.; funding acquisition, M.M.A.K. All authors have read and agreed to the published version of the manuscript.

## Funding

This research received no external funding.

## Conflicts of Interest

The authors declare no conflict of interest.

## References

- Abdullah, S.N., Kechik, M.M.A., Kamarudin, A.N., Talib, Z.A., Baqiah, H., Kien, C.S., Pah, L.K., Abdul Karim, M.K., Shabdin, M.K., Shaari, A.H., Hashim, A., Suhaimi, N.E., & Miryala, M. (2023). Microstructure and Superconducting Properties of Bi-2223 Synthesized via Co-Precipitation Method: Effects of Graphene Nanoparticle Addition. *Nanomaterials*, *13*(15). <http://dx.doi.org/10.3390/nano13152197>
- Adetokun, B.B., Oghorada, O., & Abubakar, S.J. (2022). Superconducting magnetic energy storage systems: Prospects and challenges for renewable energy applications. *Journal of Energy Storage*, *55*(PC), 105663. <https://doi.org/10.1016/j.est.2022.105663>
- Arlina, A., Halim, S. A., Kechik, M.M.A., & Chen, S.K. (2015). Superconductivity in Bi-Pb-Sr-Ca-Cu-O ceramics with YBCO as additive. *Journal of Alloys and Compounds*, *645*, 269–273. <https://doi.org/10.1016/j.jallcom.2015.04.133>
- Cheng, Y., Zheng, J., Huang, H., & Deng, Z. (2021). A reconstructed three-dimensional HTS bulk electromagnetic model considering J spatial inhomogeneity and its implementation in a bulks'

- combination system. *Superconductor Science and Technology*, 34(12).  
<http://dx.doi.org/10.1088/1361-6668/ac336b>
- Darsono, N., Imaduddin, A., & Raju, K. (2015). Synthesis and Characterization of  $\text{Bi}_{1.6}\text{Pb}_{0.4}\text{Sr}_2\text{Ca}_2\text{Cu}_3\text{O}_7$  Superconducting Oxide by High-Energy Milling. *Journal of Superconductivity and Novel Magnetism*, 28(8):1-8  
<http://dx.doi.org/10.1007/s10948-015-3036-3>
- Dihom, M.M., Halim, S.A., Baqiah, H., Mohammed Al-Hada, N., Talib, Z.A., Chen, S.K., Azis, R.S., Kechik, M.M.A., Lim, K.P. & Abd-Shukor, R. (2017). Structural and superconducting properties of  $\text{Y}(\text{Ba}_{1-x}\text{K}_x)_2\text{Cu}_3\text{O}_{7-\delta}$  ceramics. *Ceramics International*, 43(14), 11339-11344.  
<https://doi.org/10.1016/j.ceramint.2017.05.339>
- Dogruer, M., Aksoy, C., Yildirim, G., Ozturk, O., & Terzioğlu, C. (2021). Influence of Sr/Nd partial replacement on fundamental properties of Bi-2223 superconducting system. *Journal of Materials Science: Materials in Electronics*, 32(6), 7073-7089.  
<http://dx.doi.org/10.1007/s10854-021-05417-4>
- Dzul-Kifli, N.A.C., Kechik, M.M.A., Baqiah, H., Shaari, A.H., Lim, K.P., Chen, S.K., Sukor, S.I.A., Shabdin, M.K., Karim, M.K.A., Shariff, K.K.M., & Miryala, M. (2022). Superconducting Properties of  $\text{YBa}_2\text{Cu}_3\text{O}_{7-\delta}$  with a Multiferroic Addition Synthesized by a Capping Agent-Aided Thermal Treatment Method. *Nanomaterials*, 12(22).  
<http://dx.doi.org/10.3390/nano12223958>
- Hapipi, N.M., Chen, S.K., Shaari, A.H., Kechik, M.M.A., Tan, K.B., & Lim, K.P. (2018). Superconductivity of  $\text{Y}_2\text{O}_3$  and  $\text{BaZrO}_3$  nanoparticles co-added  $\text{YBa}_2\text{Cu}_3\text{O}_{7-\delta}$  bulks prepared using co-precipitation method. *Journal of Materials Science: Materials in Electronics*, 29(21), 18684-18692.  
<https://link.springer.com/article/10.1007/s10854-018-9991-2>
- Kamarudin, A.N., Awang Kechik, M.M., Abdullah, S.N., Baqiah, H., Chen, S.K., Abdul Karim, M.K., Ramli, A., Lim, K.P., Shaari, A.H., Miryala, M., Murakami, M., & Talib, Z.A. (2022). Effect of Graphene Nanoparticles Addition on Superconductivity of  $\text{YBa}_2\text{Cu}_3\text{O}_{7-\delta}$  Synthesized via the Thermal Treatment Method. *Coatings*, 12(1), 91.  
<https://doi.org/10.3390/coatings12010091>
- Kameli, P., Salamati, H., & Eslami, M. (2006). The effect of sintering temperature on the intergranular properties of Bi2223 superconductors. *Solid State Communications*, 137(1-2), 30-35.  
<https://doi.org/10.1016/j.ssc.2005.10.026>
- Kavitha, M., Sarvesh, S., Arshad, M., Surendar, M., & Ragavan, G. (2024). Effect of Ba and Mg Substitution on the Phase Formations of Combustion Synthesized BSCCO Superconductor. *Journal of The Institution of Engineers (India): Series D*.  
<http://dx.doi.org/10.1007/s40033-023-00634-z>
- Kechik, M.M.A., Aris, M.F.M., Shaari, A.H., Chen, S.K. and Roslan, A.S. (2008). Addition of  $\text{Co}_3\text{O}_4$  to Introduce Pinning Centre in Bi-Sr-Ca-Cu-O/Ag Tapes. *Pertanika Journal of Science & Technology*, 16, 259-263.
- Khalil, S.M., & Sedky, A. (2005). Annealing temperature effect on the properties of Bi:2212 superconducting system. *Physica B: Condensed Matter*, 357(3-4), 299-304. <https://doi.org/10.1016/j.physb.2004.11.080>
- Maeda, H., Tanaka, Y., Fukutomi, M., & Asano, T. (1993). A New High-T<sub>c</sub> Oxide Superconductor without a Rare Earth Element. *Physica C: Superconductivity*, 209, 303-304. [https://doi.org/10.1016/0921-4534\(88\)90727-7](https://doi.org/10.1016/0921-4534(88)90727-7)
- Matsushita, T., Kiuchi, M., Nishijima, G., Masuda, T., Mukoyama, S., Aoki, Y., & Nakai, A. (2021). Round Robin Test of Critical Current of Superconducting Cable. *IEEE Transactions on Applied Superconductivity*, 31(5), 26-29.  
<http://dx.doi.org/10.1109/TASC.2021.3058232>
- Sekkina, M.M.A., & Elsabay, K.M. (2002). Sr-doping for promoted high-T<sub>c</sub> BPSCCO superconductors. *Physica C: Superconductivity and Its Applications*, 377(3), 254-259. [https://doi.org/10.1016/S0921-4534\(02\)01250-9](https://doi.org/10.1016/S0921-4534(02)01250-9)
- Sharma, D., Kumar, R., & Awana, V.P.S. (2013). DC and AC susceptibility study of sol-gel synthesized  $\text{Bi}_2\text{Sr}_2\text{CaCu}_2\text{O}_{8+\delta}$  superconductor. *Ceramics International*, 39(2), 1143-1152.  
<https://doi.org/10.1016/j.ceramint.2012.07.038>
- Siregar, D.R.D.K., Yudianto, S.D., Chandra, S.A., Lubis, E.F.R., Humaidi, S., & Darsono, N. (2021). Improvement of the superconducting properties of carbon addition on  $\text{Bi}_{1.6}\text{Pb}_{0.4}\text{Sr}_2\text{Ca}_2\text{Cu}_3\text{O}_{10+\delta}$  prepared through the two-step sintering process. *Journal of Metals, Materials and Minerals*, 31(4), 76-81.  
<http://dx.doi.org/10.14456/jmmm.2021.60>
- Sugawara, K., Sugimoto, C., Luo, T., Kawamata, T., Noji, T., Kato, M., & Koike, Y. (2018). Superconductivity above 100 K in the Bi-2212 phase of  $(\text{Bi,Pb})_2\text{Sr}_2\text{CaCu}_2\text{O}_8$ . *Journal of Physics: Conference Series*, 1054(1).
- Sukor, S.I.A., Kechik, M.M.A., Kamarudin, A.N., Shaari, A.H., Kien, C.S., Pah, L.K., Shariff, K.K.M., Shabdin, M.K., Yaakob, Y., Karim, M.K.A., & Doyan, A. (2024). Influence of Carbon Nanotubes in Improving the Superconducting and Structural Properties of Bulk Bi-2212 Synthesis by Thermal Treatment Method. *AMPLITUDO : Journal of Science and Technology Innovation*, 3(2), 117-122.  
<http://dx.doi.org/10.56566/amplitudo.v3i2.224>
- Tsukamoto, T., Triscone, G., Genoud, J.Y., Wang, K.Q., Janod, E., Junod, A., & Müller, J. (1994). Preparation

and superconducting properties of high-quality Bi-2212 ceramics. *Journal of Alloys and Compounds*, 209(1-2), 225-229. [https://doi.org/10.1016/0925-8388\(94\)91103-7](https://doi.org/10.1016/0925-8388(94)91103-7)

Zahari, R.M., Shaari, A.H., Abbas, Z., Baqiah, H., Chen, S.K., Lim, K.P., & Kechik, M.M.A. (2017). Simple preparation and characterization of bismuth ferrites nanoparticles by thermal treatment method. *Journal of Materials Science: Materials in Electronics*, 28(23), 17932-17938. <https://link.springer.com/article/10.1007/s10854-017-7735-3>

Zhai, Y., Otto, A., & Zarnstorff, M. (2022). Low cost, simpler HTS cable conductors for fusion energy systems. *IOP Conference Series: Materials Science and Engineering*, 1241(1), 012023. <http://dx.doi.org/10.1088/1757-899X/1241/1/012023>